Network analysis of resting-state fMRI reveals increased centrality in regions generating focal epileptiform spikes

Richard Masterton[1], and Graeme Jackson[1,2]

[1]*Brain Research Institute, Florey Neuroscience Institutes, Melbourne, Victoria, Australia,* [2]*The University of Melbourne, Melbourne, Victoria, Australia*

Introduction: The seizures of patients with focal epilepsy arise from a focal region in the brain (the "epileptogenic" zone) that recruits and spreads into more widespread networks, resulting in the outward clinical manifestations of the seizure. Resting-state functional connectivity, which can identify networks in the brain based upon correlated low-frequency co-fluctuations, offers the possibility to measure these epileptogenic networks. Recent resting-state fMRI studies have reported more widespread functional connectivity networks for epileptogenic versus non-epileptogenic brain regions (1,2) and that epileptogenic regions exert significant influence upon non-epileptogenic regions during the interictal period (3). These studies suggest that these properties – i.e. increased functional connectivity and directed influence upon other brain regions – may provide useful markers to localise and identify possible epileptogenic brain regions from whole-brain functional connectivity measurements.

In this study, we used the PageRank algorithm (4) to analyse resting-state fMRI in a group of patients with benign rolandic epilepsy – a non-lesional focal epilepsy syndrome. PageRank provides a measure of node centrality (5) for directed graphs, and we hypothesised that epileptogenic regions would show high centrality in the brain's functional connectivity networks due to the properties listed above.

Methods: Twenty-six patients and 16 age-matched controls were studied. For each subject, five minutes of eyes-closed resting-state fMRI was used for analysis (TR=3000 ms; TE=40 ms; FOV=24×24 cm; 128×128 matrix; 25 slices). The fMRI data were pre-processed (slice acquisition time correction; motion realignment; spatial normalisation; Gaussian spatial smoothing; and temporal high-pass filtering (0.01 Hz)) and physiological noise was estimated and removed from the data using the average signal within white matter and CSF and the motion realignment parameters.

Functional connectivity networks were estimated by comparing all pairs of voxels within the brain. A two-step process was used: first a test was performed to select voxel pairs that were functionally connected, and then the "direction" of the connection between these voxel pairs was estimated. The presence of a connection was inferred when the Pearson's correlation coefficient between band-pass filtered (0.01-0.1 Hz) voxel time-courses exceeded a threshold value of r = 0.4. The directionality of functional connections was estimated with Granger causality (6), using the difference between F statistics to infer the direction of causality (7).

All functional connectivity and causality estimation was performed using multi-subject temporally-concatenated data to minimise the effect of regional haemodynamic response variability upon causality estimation. This approach was taken because the spatial variation in haemodynamic response shape is markedly reduced in measurements that are averaged across groups of subjects (8), which suggests the variability is random rather than regionally correlated, and that intra-voxel timing differences arising purely from haemodynamic variability should therefore be reduced in multi-subject data (9,10). A bootstrapping procedure was used, with 25 random samples of 15 subjects drawn from the data (with replacement), and each sample temporally-concatenated. Before temporal concatenation each subject's voxel time-series were normalised to zero mean and unit variance.

The estimated functional connectivity relationships were represented as a directed graph, and the centrality of each node was estimated using the PageRank algorithm (4).

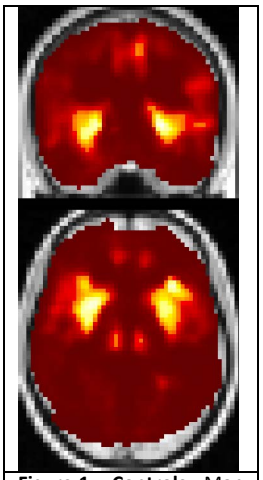

Figure 1 – Controls: Map showing the mean PageRank centrality in the patient group. Hot colours indicate regions with high centrality.

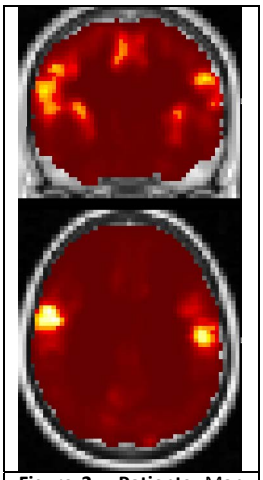

Figure 2 – Patients: Map showing the mean PageRank centrality in the patient group. Hot colours indicate regions with high centrality.

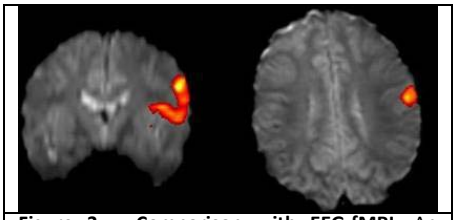

Figure 3 – Comparison with EEG-fMRI: An example EEG-fMRI activation map from a single subject, showing activation in the left inferior post-central gyrus in association with left-sided rolandic spikes.

Results & Discussion: The analysis of resting-state functional connectivity networks revealed marked differences between the two groups, with the controls showing highest centrality in the basal ganglia, insula cortex and thalamus, whereas the epilepsy patients showed highest centrality bilaterally in the post-central gyrus (Figures 1 & 2). The centrality of the post-central gyrus was significantly greater ($p < 0.05$, corrected) in the patients, and this region has also been shown to activate during the epileptiform spikes of rolandic epilepsy (11). For comparison purposes, data from a subject who had left-sided rolandic spikes on simultaneous EEG during the fMRI study is provided in Figure 3, showing spike-related activation in the left inferior post-central gyrus. This concordance between the region of high centrality and the region generating epileptiform discharges suggests that PageRank centrality of resting-state fMRI networks may provide a data-driven approach for localising epileptogenic brain regions in focal epilepsy. Importantly, this may provide an alternative to the EEG-fMRI approach, particularly in the 40-70% of EEG-fMRI studies that fail due to insufficient epileptiform activity being detected on the scalp-recorded EEG (12).

References:

1. Archer JS, et al. Epilepsy Behav. 2010; 19(4):631–4.
2. Stufflebeam SM, et al. J Neurosurg 2011 http://dx.doi.org/10.3171/2011.1.JNS10482
3. Bettus G, et al. PLoS One. 2011;6(5):e20071.
4. Brin S, Page L.. Comput Networks ISDN. 1998;30(1-7):107–17.
5. Freeman LC. Soc Networks. 1979;1(3):215–39.
6. Goebel R, et al. Magn Reson Imaging. 2003;21(10):1251–61.
7. Roebroeck A, et al. Neuroimage. 2005;25(1):230–42.
8. Lin F-H, et al. Neuroimage. 2010;49(4):3086–98.
9. Schippers MB, et al. Neuroimage. 2011;57(1):22–36.
10. Ramsey JD, et al. NeuroImage. 2011;58(3):838–48.
11. Masterton RAJ, et al. Neuroimage. 2010; 51:252–60.
12. Grouiller F, et al. Brain. 2011. http://brain.oxfordjournals.org/content/early/2011/07/12/brain.awr156.abstract